

Tetranuclear Clusters Containing a Cr^{III}-Doped Mn^{II}₄O₂ Core: Syntheses, Structures, and Magnetic Properties

Yun-Sheng Ma, Yi-Zhi Li, You Song, and Li-Min Zheng*

State Key Laboratory of Coordination Chemistry, Coordination Chemistry Institute, School of Chemistry and Chemical Engineering, Nanjing University, Nanjing 210093, People's Republic of China

Received August 16, 2007

The oxidation of Mn^{II} carboxylates by (NBu₄)Cr₂O₇ in the presence of different phosphonic acids and chelating ligands results in six Cr^{III}-doped tetranuclear manganese clusters formulated [Mn₃CrO₂(O₂CCH₃)₄(O₃PC₅H₄N)₂(bpy)₂] (1), [Mn₃CrO₂(O₂CCH₃)₄(O₃PC₅H₄N)₂(phen)₂] (2), [Mn₃CrO₂(O₂CPh)₄(O₃PC₅H₄NO)₂(phen)₂] (3), [Mn₃CrO₂(O₂CPh)₄(O₃PC₆H₁₁)₂(bpy)₂] (4), [Mn₃CrO₂(O₂CPh)₄(O₃PC₆H₁₁)₂(phen)₂] (5), and [Mn₃CrO₂(O₂CCH₃)₄(O₃PC₆H₁₁)₂(bpy)₂] (6). Single-crystal X-ray analyses reveal that all the compounds contain similar [M₄O₂]⁸⁺ cores with the four metal sites arranged in planar topologies. The metal ions within the core are bridged by both carboxylate and phosphonate ligands. Temperature-dependent magnetic measurements show that in all cases dominant antiferromagnetic interactions are propagated between the metal centers. The ac magnetic measurements on compounds 5 and 6 reveal that both the in-phase and the out-of-phase signals are frequency dependent, characteristic of single-molecule magnet behaviors.

Introduction

Oxo-bridged tetranuclear manganese clusters have been of great interest as models to mimic the water oxidation center of photosystem II and as molecular based magnetic materials.^{1–3} It is well-known that single-molecule magnets (SMMs) are molecules that can be magnetized in a magnetic field and retain the magnetization when it is switched off. As a consequence, they may show hysteresis loops reminiscent of magnets and may exhibit slow magnetic relaxation at low temperatures.⁴ The slow relaxation of the magnetization is closely associated with their intrinsic properties of a high-spin ground state (S_T), a high uniaxial anisotropy (negative zero-field splitting parameter, D), and a small transverse anisotropy. These characteristics create an energy barrier, ΔE , lying between “spin-up” and “spin-down” states that must be overcome to reverse the spin direction. So far, there are a number of oxo-bridged homovalent or mixed-

valent Mn₄ clusters reported, many of which possess a planar or butterfly-like (Mn₄O₂)ⁿ⁺ ($n = 6, 7, \text{ or } 8$) core.⁵ The ground-state spin of these complexes varies depending on their structures and the spin-frustration effect involved in such systems.⁶ In order to obtain single-molecule magnets of this type with a high ground-state spin, Mn₄ clusters containing cube-like cores are designed and synthesized, which allow for the ferromagnetic exchange couplings between the Mn centers.^{7–10}

Another approach that has been less explored is to introduce a second metal into the tetranuclear cores. Very few mixed-metal tetranuclear compounds with planar or

* To whom correspondence should be addressed. E-mail: lmzheng@netra.nju.edu.cn. Fax: +86-25-83314502.

- (1) Wieghardt, K. *Angew. Chem., Int. Ed. Engl.* **1989**, *28*, 1153.
- (2) Rüttinger, W.; Dismukes, G. C. *Chem. Rev.* **1997**, *97*, 1.
- (3) Christou, G. *Acc. Chem. Res.* **1989**, *22*, 328.
- (4) (a) Sessoli, R.; Tsai, H.-L.; Schake, A. R.; Wang, S.; Vincent, J. B.; Folting, K.; Gatteschi, D.; Christou, G.; Hendrickson, D. N. *J. Am. Chem. Soc.* **1993**, *115*, 1804. (b) Sessoli, R.; Gatteschi, D.; Caneschi, A.; Novak, M. A. *Nature* **1993**, *365*, 141.

- (5) Aromí, G.; Brechin, E. K. *Struct. Bond.* **2006**, *122*, 1.
- (6) (a) Albela, B.; Fallah, M. S. E.; Ribas, J.; Folting, K.; Christou, G.; Hendrickson, D. N. *Inorg. Chem.* **2001**, *40*, 1037. (b) Wemple, M. W.; Tsai, H. L.; Wang, S.; Claude, J. P.; Streib, W. E.; Huffman, J. C.; Hendrickson, D. N.; Christou, G. *Inorg. Chem.* **1996**, *35*, 6437.
- (7) Aliaga-Alcalde, N.; Edwards, R. S.; Hill, S. O.; Wernsdorfer, W.; Folting, K.; Christou, G. *J. Am. Chem. Soc.* **2004**, *126*, 12503.
- (8) (a) Brechin, E. K.; Yoo, J.; Nakano, M.; Huffman, J. C.; Hendrickson, D. N.; Christou, G. *Chem. Commun.* **1999**, 783. (b) Yoo, J.; Brechin, E. K.; Yamaguchi, A.; Nakano, M.; Huffman, J. C.; Maniero, A. L.; Brunel, L.; Awaga, K.; Ishimoto, H.; Christou, G.; Hendrickson, D. N. *Inorg. Chem.* **2000**, *39*, 3615. (c) Aubin, S. M. J.; Dilley, N. R.; Pardi, L.; Krzystek, J.; Wemple, M. W.; Brunel, L.-C.; Maple, M. B.; Christou, G.; Hendrickson, D. N. *J. Am. Chem. Soc.* **1998**, *120*, 4991.
- (9) Milios, C. J.; Prescimone, A.; Mishra, A.; Parsons, S.; Wernsdorfer, W.; Christou, G.; Perlepes, S. P.; Brechin, E. K. *Chem. Commun.* **2007**, 153.

butterfly-like cores have been described in the literature.^{11–13} Chaudhuri et al. reported complex [L₂Cr₂(μ-OMe)₂(μ₃-O)₂-(salox)₂Mn₂][ClO₄]₂·3H₂O containing a butterfly-like [Cr^{III}₂-Mn^{III}₂O₂]⁸⁺ core, in which Cr^{III} ions occupy the wingtip metal sites.¹¹ The ground state of this complex turns out to be S_T = 0. The same research group also prepared a series of Fe^{III}-Mn^{III} complexes with the formula [L₂Fe₂(μ₃-O)₂-(salox)₂(O₂CR)₃Mn₂](ClO₄), which possess a similar butterfly-like [Fe^{III}₂Mn^{III}₂O₂]⁸⁺ core.¹² The two Fe^{III} ions are again residing on the wingtip sites. Interestingly, the ground-state spin of these complexes varies from S_T = 1 to S_T = 3 by changing the bridging carboxylates in the [Fe₂Mn₂O₂] core from acetate to diphenylglycolate, triphenyl acetate, benzoate, chloroacetate, and propionate, due to spin frustration of the “body” manganese centers. Benelli et al. reported the complexes [Mn₂Ln₂O₂(O₂CCMe₃)₈(HO₂CCMe₃)₂(MeOH)₂] (Ln = Gd, Dy) containing a distorted butterfly core of [Mn^{III}₂Ln^{III}₂O₂]⁸⁺.¹³ The magnetic behavior of the Mn^{III}-Gd^{III} complex is dominated by strong antiferromagnetic coupling between the dioxo-bridged Mn(III) centers and by ferromagnetic coupling between Mn and Gd. None of these complexes displays magnetic behaviors characteristic of a single-molecule magnet. Slow relaxation behavior or even a magnetization hysteresis loop has been observed in Mn^{III}₂Ni^{II}₂ and Mn^{III}₂Ln^{III}₂ clusters where incomplete double-cubane cores are found.^{14,15}

It is noticed that, in these heteronuclear complexes, the molar ratio of the two kinds of metal atoms remains 2:2. If we could change the molar ratio into 1:3, modifications on both the structural parameters and the magnetic behaviors are expected. To fulfill this purpose, we develop a new synthetic route, by using (NBu₄)₂Cr₂O₇ to oxidize Mn^{II} in situ, resulting in six new heteronuclear complexes with a general formula [Mn₃CrO₂(O₂CR¹)₄(O₃PR²)₂(L)₂] (R¹ = CH₃, Ph; R² = C₅H₄N, C₅H₄NO, C₆H₁₁; L = bpy, phen). Some of them show slow relaxation phenomena characteristic of single-molecule magnets.

Experimental Section

Materials and Methods. All experiments were conducted under aerobic conditions, using materials as received. 2-Pyridylphosphonic acid (2-C₅H₄NPO₃H₂),¹⁶ (2-pyridyl-*N*-oxide)phosphonic acid (2-C₅H₄NOPO₃H₂),¹⁷ cyclohexanephosphonic acid (C₆H₁₁PO₃H₂),¹⁸

and (NBu₄)₂Cr₂O₇¹⁹ were prepared according to the literature. Elemental analyses for C, H, and N were performed in a PE 240C elemental analyzer. The metal contents were analyzed on a J-A1100 ICP-AES (inductively coupled plasma-atomic emission spectroscopy) instrument. The IR spectra were recorded on a VECTOR 22 spectrometer with pressed KBr pellets. Thermal analyses were performed in nitrogen with a heating rate of 10 °C/min on a PerkinElmer Pyris 1 TGA (thermogravimetric analysis) instrument. Variable-temperature magnetic susceptibility data were obtained on polycrystalline samples using a Quantum Design MPMS-XL7 SQUID (superconducting quantum interference device) magnetometer. The data were corrected for the diamagnetic contributions of both the sample holder and the compound obtained from Pascal's constants.²⁰

Preparation of [Mn₃CrO₂(O₂CCH₃)₄(O₃PC₅H₄N)₂(bpy)₂]·4CH₃-OH (1·4CH₃OH). To a solution of Mn(O₂CCH₃)₂·4H₂O (0.20 g, 0.815 mmol) and CH₃CO₂H (2 mmol) in 10 mL of CH₃OH and 10 mL of CH₂Cl₂ was added (NBu₄)₂Cr₂O₇ (0.117 g, 0.167 mmol) in small portions. After 20 min of stirring, 2-pyridylphosphonic acid (0.088 g, 0.5 mmol) and bpy (0.078 g, 0.5 mmol) were added, and the mixture was stirred for an additional 24 h. The resulting red-brown solution was filtered, and the black crystals of 1·4CH₃OH were isolated from the filtrate after 7 days. Yield: 0.139 g (33.6% based on (NBu₄)₂Cr₂O₇). Elemental analyses calcd (%) for C₄₂H₅₂CrMn₃N₆O₂₀P₂: C, 40.69; H, 4.23; N, 6.78; Mn, 13.30; Cr, 4.19. Found: C, 40.57; H, 4.14; N, 6.73; Mn, 13.50; Cr, 3.4. IR (cm⁻¹, KBr): 3422 (br), 1581 (s), 1496 (w), 1444 (s), 1420 (s), 1192 (m), 1162 (m), 1024 (m), 961 (m), 770 (m), 737 (m), 663 (s), 618 (m), 521 (m), 486 (w). Thermogravimetric analysis shows a one-step weight loss (10.43%) in the temperature range 20–120 °C, which is in agreement with the calculated value of 10.32% for the removal of four CH₃OH molecules.

Preparation of [Mn₃CrO₂(O₂CCH₃)₄(O₃PC₅H₄N)₂(phen)₂]·2CH₃OH·2.5H₂O (2·2CH₃OH·2.5H₂O). Compound 2 was prepared following a similar procedure to that for the preparation of 1 except that bpy was replaced by phen. Yield: 0.143 g (33.7% based on (NBu₄)₂Cr₂O₇). Elemental analyses calcd (%) for C₄₄H₄₉-CrMn₃N₆O_{20.5}P₂: C, 41.66; H, 3.89; N, 6.62; Mn, 12.99; Cr, 4.10. Found: C, 41.56; H, 3.78; N, 6.60; Mn, 13.40; Cr, 3.25. IR (cm⁻¹, KBr): 3421 (br), 1577 (s), 1520 (m), 1429 (s), 1345 (w), 1191 (m), 1164 (m), 1026 (m), 963 (m), 854 (w), 781 (w), 728 (m), 657 (m), 610 (m), 522 (m), 489 (w). Thermogravimetric analysis shows a one-step weight loss (9.03%) in the temperature range 20–120 °C, which is in agreement with the calculated value of 8.59% for the removal of 2 CH₃OH molecules and 2.5 water molecules.

Preparation of [Mn₃CrO₂(O₂CPh)₄(O₃PC₅H₄NO)₂(phen)₂]·4CH₃OH·2H₂O (3·4CH₃OH·2H₂O). Compound 3 was prepared following a similar procedure to that for the preparation of 1 but using Mn(O₂CPh)₂·2H₂O, HO₂CPh, (NBu₄)₂Cr₂O₇, (2-pyridyl-*N*-oxide)phosphonic acid, and phen as starting materials. Yield: 0.164 g (30.6% based on (NBu₄)₂Cr₂O₇). Elemental analyses calcd (%) for C₆₆H₆₄CrMn₃N₆O₂₄P₂: C, 49.42; H, 4.02; N, 5.24; Mn, 10.28; Cr, 3.24. Found: C, 49.11; H, 3.11; N, 5.68; Mn, 10.2; Cr, 3.33. IR (cm⁻¹, KBr): 3416 (br), 3063 (m), 1603 (s), 1566 (s), 1520 (m), 1426 (s), 1398 (s), 1266 (w), 1215 (m), 1178 (m), 1149 (m), 1106 (w), 1068 (m), 1025 (m), 974 (m), 847 (m), 778 (w), 722 (s), 670 (s), 599 (m), 535 (m), 507 (m), 461 (w). Thermogravimetric analysis shows a one-step weight loss (9.67%) in the temperature range

- (10) (a) Ako, A. M.; Mereacre, V.; Hewitt, I. J.; Clérac, R.; Lecren, L.; Anson, C. E.; Powell, A. K. *J. Mater. Chem.* **2006**, *16*, 2579. (b) Lecren, L.; Roubeau, O.; Coulon, C.; Li, Y.-G.; Le Goff, X. F.; Wernsdorfer, W.; Miyasaka, H.; Clérac, R. *J. Am. Chem. Soc.* **2005**, *127*, 17353.
 (11) Chaudhuri, P.; Birkelbach, F.; Winter, M.; Staemmler, V.; Fleischhauer, P.; Haase, W.; Flörke, U.; Haupt, H.-J. *J. Chem. Soc., Dalton Trans.* **1994**, 2313.
 (12) Chaudhuri, P.; Rentschler, E.; Birkelbach, F.; Krebs, C.; Bill, E.; Weyhermüller, T.; Flörke, U. *Eur. J. Inorg. Chem.* **2003**, 541.
 (13) Benelli, C.; Murrie, M.; Parsons, S.; Winpenny, R. E. P. *J. Chem. Soc., Dalton Trans.* **1999**, 4125.
 (14) Oshio, H.; Nihei, M.; Koizumi, S.; Shiga, T.; Nojiri, H.; Nakano, M.; Shirakawa, N.; Akatsu, M. *J. Am. Chem. Soc.* **2005**, *127*, 4568.
 (15) Mishra, A.; Wernsdorfer, W.; Parsons, S.; Christou, G.; Brechin, E. K. *Chem. Commun.* **2005**, 2086.
 (16) Loran, J. S.; Naylor, R. A.; Williams, A. J. *Chem. Soc., Perkin Trans. 2* **1976**, *12*, 1444.
 (17) McCabe, D. J.; Russell, A. A.; Karthikeyan, S.; Paine, R. T.; Ryan, R. R.; Smith, B. *Inorg. Chem.* **1987**, *26*, 1230.

(18) Clayton, J. O.; Jensen, W. L. *J. Am. Chem. Soc.* **1948**, *70*, 4880.

(19) Santaniello, E.; Ferraboschi, P. *Synth. Commun.* **1980**, *10*, 75.

(20) Kahn, O. *Molecular Magnetism*; VCH Publishers, Inc.: New York, 1993.

Table 1. Crystallographic Data for 1–6

	1·4CH ₃ OH	2·2CH ₃ OH·2.5H ₂ O	3·4CH ₃ OH·2H ₂ O	4·4H ₂ O	5·4H ₂ O	6·7H ₂ O
formula	C ₄₂ H ₅₂ CrMn ₃ N ₆ O ₂₀ P ₂	C ₄₄ H ₄₉ CrMn ₃ N ₆ O _{20.5} P ₂	C ₆₆ H ₆₄ CrMn ₃ N ₆ O ₂₄ P ₂	C ₆₄ H ₆₆ CrMn ₃ N ₄ O ₂₀ P ₂	C ₆₀ H ₆₆ CrMn ₃ N ₄ O ₂₀ P ₂	C ₄₀ H ₆₄ CrMn ₃ N ₄ O ₂₃ P ₂
mol wt	1239.66	1268.65	1603.99	1489.97	1441.93	1247.71
cryst syst	monoclinic	monoclinic	triclinic	monoclinic	monoclinic	triclinic
space group	<i>P</i> 2 ₁ / <i>c</i>	<i>P</i> 2 ₁ / <i>c</i>	<i>P</i> $\bar{1}$	<i>P</i> 2 ₁ / <i>n</i>	<i>P</i> 2 ₁ / <i>c</i>	<i>P</i> $\bar{1}$
<i>a</i> (Å)	13.409(3)	20.972(4)	10.796(2)	12.060(9)	12.019(3)	11.302(2)
<i>b</i> (Å)	13.263(3)	13.156(3)	14.295(2)	18.215(13)	12.766(3)	11.759(2)
<i>c</i> (Å)	14.712(3)	21.413(4)	14.649(3)	16.835(12)	24.367(5)	12.199(2)
α (deg)	90	90	111.586(3)	90	90	100.85(3)
β (deg)	106.16(3)	115.94(3)	110.370(3)	97.05(2)	90.31(1)	99.55(3)
γ (deg)	90	90	96.781(3)	90	90	116.71(3)
vol (Å ³)	2513.1(10)	5312.7(18)	1890.6(6)	3670(5)	3738.6(14)	1363.1(7)
<i>Z</i>	2	4	1	2	2	1
<i>D</i> _{calcd} (g·cm ⁻³)	1.638	1.586	1.409	1.348	1.281	1.520
μ (Mo K α) (mm ⁻¹)	1.094	1.038	0.749	0.761	0.745	1.011
<i>F</i> (000)	1270	1296	823	1534	1486	643
total, unique data	12483, 4882	27724, 10432	10241, 7238	19506, 7153	21241, 8064	12695, 5342
<i>R</i> _{int}	0.039	0.035	0.033	0.038	0.052	0.030
observed data	3291	7966	5125	5249	5362	4506
<i>R</i> ₁ , ^a <i>R</i> ₂ ^b	0.053, 0.084	0.055, 0.111	0.063, 0.126	0.051, 0.091	0.054, 0.108	0.055, 0.123
GOF ^c	1.06	1.05	1.07	1.05	1.02	1.01
$\Delta\rho_{\max}$, $\Delta\rho_{\min}$ (e·Å ⁻³)	0.43, -0.35	0.27, -0.65	0.60, -0.65	0.24, -0.27	0.27, -0.31	0.31, -0.51

$$^a R_1 = \sum |F_o| - |F_c| / \sum |F_o|, \quad ^b R_2 = [\sum w(F_o^2 - F_c^2)^2 / \sum w(F_o^2)^2]^{1/2}, \quad ^c \text{GOF} = [\sum [w(F_o^2 - F_c^2)^2] / (N_{\text{obs}} - N_{\text{param}})]^{1/2}.$$

20–120 °C, which is in agreement with the calculated value of 10.22% for the removal of four CH₃OH molecules and two water molecules.

Preparation of [Mn₃CrO₂(O₂CPh)₄(O₃PC₆H₁₁)₂(bpy)₂]·4H₂O (4·4H₂O). Compound **4** was prepared following a similar procedure to that for the preparation of **3** except that cyclohexanephosphonic acid and bpy were used as starting materials and CH₃CN and CH₂Cl₂ were used as solvents. Yield: 0.190 g (39.5% based on (NBu₄)₂Cr₂O₇). Elemental analyses calcd (%) for C₆₀H₆₆CrMn₃N₄O₂₀P₂: C, 49.98; H, 4.61; N, 3.88; Mn, 11.43; Cr, 3.61. Found: C, 49.51; H, 4.59; N, 3.94; Mn, 10.90; Cr, 3.20. IR (cm⁻¹, KBr): 3427 (br), 3065 (w), 2930 (m), 2852 (w), 1597 (s), 1561 (s), 1498 (w), 1471 (w), 1447 (m), 1400 (s), 1084 (m), 1024 (m), 989 (m), 944 (s), 773 (m), 719 (s), 678 (m), 657 (m), 599 (m), 568 (m), 464 (m). Thermogravimetric analysis shows a one-step weight loss (5.05%) in the temperature range 20–120 °C, which is in agreement with the calculated value of 4.99% for the removal of four water molecules.

Preparation of [Mn₃CrO₂(O₂CPh)₄(O₃PC₆H₁₁)₂(phen)₂]·4H₂O (5·4H₂O). Compound **5** was prepared following a similar procedure to that for the preparation of **4** except that bpy was replaced by phen. Yield: 0.198 g (39.8% based on (NBu₄)₂Cr₂O₇). Elemental analyses calcd (%) for C₆₄H₆₆N₄O₂₀P₂CrMn₃: C, 51.59; H, 4.46; N, 3.76; Mn, 11.06; Cr, 3.49. Found: C, 51.25; H, 4.41; N, 4.12; Mn, 10.8; Cr, 3.25. IR (cm⁻¹, KBr): 3422 (br), 3062 (w), 2931 (m), 2851 (w), 1596 (s), 1561 (s), 1519 (m), 1448 (w), 1400 (s), 1108 (m), 1024 (m), 982 (m), 940 (m), 875 (w), 849 (m), 721 (s), 677 (m), 659 (m), 646 (m), 599 (m), 568 (m), 464 (m). Thermogravimetric analysis shows a one-step weight loss (3.48%) in the temperature range 20–120 °C, which is lower than the calculated value of 4.83% for the removal of four water molecules.

Preparation of [Mn₃CrO₂(O₂CCH₃)₄(O₃PC₆H₁₁)₂(bpy)₂]·7H₂O (6·7H₂O). Compound **6** was prepared following a similar procedure to that for the preparation of **4** except that Mn(O₂CCH₃)₂·4H₂O and CH₃CO₂H were replaced by Mn(O₂CPh)₂·2H₂O and PhCO₂H, respectively. Yield: 0.134 g (32.2% based on (NBu₄)₂Cr₂O₇). Elemental analyses calcd (%) for C₄₀H₆₄CrMn₃N₄O₂₃P₂: C, 38.50; H, 5.17; N, 4.49; Mn, 13.21; Cr, 4.17. Found: C, 38.49; H, 4.99; N, 4.43; Mn, 13.60; Cr, 4.38. IR (cm⁻¹, KBr): 3428 (br), 2930

(m), 2853 (w), 1575 (s), 1498 (w), 1471 (w), 1446 (s), 1419 (s), 1340 (m), 1083 (m), 1022 (m), 978 (m), 947 (s), 777 (m), 732 (w), 666 (m), 654 (m), 598 (m), 464 (w). Thermogravimetric analysis shows a one-step weight loss (10.30%) in the temperature range 20–120 °C, which is in agreement with the calculated value of 10.10% for the removal of seven water molecules.

Crystallographic Studies. Single-crystal data were collected on a Bruker SMART APEX CCD diffractometer using graphite-monochromatized Mo K α radiation ($\lambda = 0.71073$ Å) at room temperature. The selected crystals were affixed to a glass capillary with mother liquid and transferred to the goniostat for data collection. The data were integrated using the Siemens SAINT program,²¹ with the intensities corrected for Lorentz factor, polarization, air absorption, and absorption due to variation in the path length through the detector faceplate. Absorption corrections were applied for all six compounds.

The structures were solved by direct methods and refined on *F*² by full-matrix least-squares using SHELXTL.²² Since the Cr and Mn atoms cannot be distinguished from the X-ray data, they are assumed to occupy the same metal sites statistically with a fixed Cr/Mn ratio of 1:3 based on the ICP results. All the non-hydrogen atoms in the compounds were refined anisotropically. All the hydrogen atoms were in calculated positions and refined isotropically. The crystallographic and the refinement details of the six compounds are in Table 1; the selected bond lengths and angles are in Tables 2–5.

Results and Discussion

Syntheses. The comproportionation reaction has been an effective route in the synthesis of manganese clusters.²³ Usually, NBu₄MnO₄ is used as the oxidizing agent to react with Mn^{II} salts, resulting in homonuclear manganese clusters. Only in a few cases, (NH₄)₂[Ce(NO₃)₆] is allowed to react

(21) SAINT, Program for Data Extraction and Reduction; Siemens Analytical X-ray Instruments: Madison, WI, 1994–1996.

(22) SHELXTL Reference Manual, version 5.0; Siemens Industrial Automation, Analytical Instruments: Madison, WI, 1995.

(23) Gatteschi, D.; Sessoli, R. *Angew. Chem., Int. Ed.* **2003**, *42*, 268.

Table 2. Selected Bond Distances (Å) and Angles (deg) for Compound **1**·4CH₃OH^a

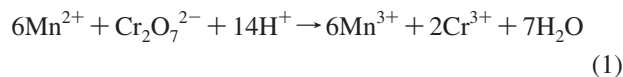
M1–O3	1.943(3)	M2–O5	1.996(3)
M1–O4	2.032(3)	M2–O6	2.129(3)
M1–O7	2.042(2)	M2–O8	1.829(3)
M1–O8	1.890(2)	M2–N2	2.222(3)
M1–N1	2.179(3)	M2–N3	2.060(3)
M1–O8A	1.989(2)	M2–O1A	1.938(2)
P1–O1	1.525(3)	P1–O2	1.472(3)
P1–O3	1.534(3)		
M1–O8–M2	122.57(12)	M1–O8–M1A	97.86(11)
M1A–O8–M2	132.41(13)		

^a Symmetry code for A: 1 – x, 2 – y, –z.**Table 3.** Selected Bond Distances (Å) and Angles (deg) for Compound **2**·2CH₃OH·2.5H₂O

M1–O4	1.936(3)	M3–O6	1.918(3)
M1–O12	1.995(2)	M3–O8	2.100(3)
M1–O14	2.105(3)	M3–O10	1.977(3)
M1–O16	1.854(2)	M3–O15	1.896(3)
M1–N1	2.056(3)	M3–O16	1.922(3)
M1–N2	2.236(3)	M3–N6	2.269(4)
M2–O2	1.979(4)	M4–O1	1.930(3)
M2–O7	2.073(3)	M4–O11	2.032(3)
M2–O9	2.012(2)	M4–O13	2.041(3)
M2–O15	1.842(3)	M4–O15	1.971(2)
M2–N3	2.216(3)	M4–O16	1.890(3)
M2–N4	2.069(3)	M4–N5	2.168(3)
P1–O4	1.530(3)	P2–O1	1.538(3)
P1–O5	1.487(3)	P2–O2	1.510(3)
P1–O6	1.522(3)	P2–O3	1.469(4)
M1–O16–M3	132.60(13)	M2–O15–M3	120.18(12)
M1–O16–M4	120.40(12)	M2–O15–M4	131.94(14)
M3–O16–M4	100.16(12)	M3–O15–M4	98.24(12)

with Mn^{II}; hence, heteronuclear Ce^{IV}–Mn^{IV} clusters are isolated.²⁴ As far as we are aware, the application of (NBu₄)₂Cr₂O₇, which is one of the well-known oxidizing agents in the organic syntheses,^{19,25} in the preparation of metal clusters has not been well explored so far. Herein, we develop a new synthetic approach to the mixed metal Mn/Cr clusters by using (NBu₄)₂Cr₂O₇ as the oxidizing agent.

Treatment of Mn(O₂CCH₃)₂·4H₂O and (NBu₄)₂Cr₂O₇ in the presence of acetic acids would generate in situ the Mn^{III} and Cr^{III} ions as shown in eq 1:



When a methanol solution of 2-pyridylphosphonic acid and bpy was added to this dark brown solution, crystals of **1**·4CH₃OH could grow and be isolated from the solution. The one-pot procedure may be extended to the preparation of compounds Mn₃CrO₂(O₂CR)₄(O₃PR')₂L₂ (R¹ = CH₃, Ph; R² = C₅H₄N, C₅H₄NO, C₆H₁₁; L = bpy, phen). In all cases, only tetranuclear clusters with a Mn/Cr molar ratio of 3:1 were obtained. The Mn/Cr molar ratio is consistent with that given in eq 1. Reactions were also carried out under other conditions by changing the molar ratio of the starting materials. For example, when the molar ratio of Mn(O₂CCH₃)₂·4H₂O, (NBu₄)₂Cr₂O₇, 2-pyridylphosphonic acid, and bpy was 1:(0.167–

Table 4. Selected Bond Distances (Å) and Angles (deg) for Compound **3**·4CH₃OH·2H₂O^a

M1–O2	1.966(3)	M2–O1	2.188(3)
M1–O3	2.089(3)	M2–O4	1.957(3)
M1–O5	1.934(3)	M2–O8	1.808(3)
M1–O8	1.926(3)	M2–N2	2.098(4)
M1–O9	2.085(3)	M2–N3	2.067(4)
M1–O8A	1.947(3)	M2–O6A	2.111(3)
P1–O5	1.514(3)	P1–O6	1.517(3)
P1–O7	1.493(4)	O9–N1	1.323(5)
M1–O8–M2	122.44(15)	M1–O8–M1A	98.28(12)
M1A–O8–M2	127.46(14)		

^a Symmetry code for A: 1 – x, 1 – y, 1 – z.**Table 5.** Selected Bond Distances (Å) and Angles (deg) for Compounds **4–6**

	4·4H ₂ O ^a	5·4H ₂ O ^b	6·7H ₂ O ^c	
M1–O2	1.929(2)	1.939(2)	M1–O2A	1.968(3)
M1–O3	1.943(2)	1.958(2)	M1–O3	1.973(3)
M1–O5	2.112(2)	2.081(3)	M1–O5A	2.109(3)
M1–O8	1.933(2)	1.931(2)	M1–O8A	1.928(3)
M1–O6A	2.119(2)	2.102(2)	M1–O6	2.102(3)
M1–O8A	1.927(2)	1.915(2)	M1–O8	1.931(3)
M2–O1	2.189(2)	2.165(3)	M2–O1	2.188(3)
M2–O7	1.881(2)	1.874(2)	M2–O7	1.882(3)
M2–O8	1.829(2)	1.832(2)	M2–O8	1.836(3)
M2–N1	2.059(3)	2.088(3)	M2–N1	2.025(4)
M2–N2	2.068(2)	2.057(3)	M2–N2	2.056(4)
M2–O4A	2.175(2)	2.170(3)	M2–O4	2.174(3)
P1–O5	1.510(2)	1.532(2)	P1–O5	1.526(3)
P1–O6	1.495(2)	1.509(2)	P1–O6	1.518(3)
P1–O7	1.547(2)	1.549(2)	P1–O7	1.547(3)
M1–O8–M2	125.79(11)	125.57(10)	M1–O8–M2	126.20(16)
M1–O8–M1A	95.21(9)	95.58(8)	M1–O8–M1A	94.92(15)
M1A–O8–M2	126.75(11)	126.33(10)	M1A–O8–M2	126.70(18)

^a Symmetry codes for A: –x, 1 – y, 1 – z. ^b Symmetry codes for A: –x, 1 – y, –z. ^c Symmetry codes for A: 1 – x, 2 – y, 1 – z.

0.333):0.5:0.5, the same compound **1**·4CH₃OH was produced together with unrecognized precipitates, or only clear solutions were obtained after keeping the mixture at room temperature for several months.

Description of Structures. Complex **1**·4CH₃OH crystallizes in the monoclinic *P*₂₁/*c* space group. Figure 1a shows the molecular structure of **1** with atomic labeling schemes. Clearly, it contains a typical [M₄(μ₃-O)₂]⁸⁺ planar core comprising four M^{III} ions, each containing ³/₄ Mn^{III} and ¹/₄ Cr^{III}. The four metal sites are arranged in a planar fashion with the central μ₃-O²⁻ ion [O(8)] deviating slightly out of this plane by 0.287(2) Å. Two M atoms are crystallographically distinguished, and both have distorted octahedral environments. The M(1) atom is surrounded by O(3) and N(1) from the same 2-pyridylphosphonate ligand, O(4) and O(7) from two acetate ligands, and two central oxygen atoms O(8) and O(8A). The M(1)–O(7) [2.042(3) Å] and M(1)–N(1) [2.179(3) Å] distances are slightly longer compared with the other M(1)–O distances [1.890(2)–2.032(3) Å]. For the M(2) atom, four of its six coordination positions are occupied by the central O(8), the acetate oxygens O(5) and O(6), and the phosphonate oxygen O(1A). The remaining two positions are filled with the nitrogen atoms [N(2) and N(3)] from bpy. The M(2)–O and M(2)–N bond lengths are in the ranges 1.829(3)–2.129(3) Å and 2.060(3)–2.222(3) Å, respectively, in which the M(2)–O(6) and the M(2)–N(2) distances are slightly longer. The elongated axes around the M(1) and the M(2) atoms, corresponding to the Jahn–Teller axes, are nearly parallel to each other.

(24) (a) Tasiopoulos, A. J.; O'Brien, T. A.; Abboud, K. A.; Christou, G. *Angew. Chem., Int. Ed.* **2004**, *43*, 345. (b) Tasiopoulos, A. J.; Wernsdorfer, W.; Moulton, B.; Zaworotko, M. J.; Christou, G. *J. Am. Chem. Soc.* **2003**, *125*, 15274.

(25) (a) Lau, T.-C.; Wang, J.; Siu, K. W. M.; Guevremont, R. *J. Chem. Soc., Chem. Commun.* **1994**, 1487. (b) Lau, T.-C.; Wu, Z.-B.; Bai, Z.-L.; Mak, C.-K. *J. Chem. Soc., Dalton Trans.* **1995**, 695.

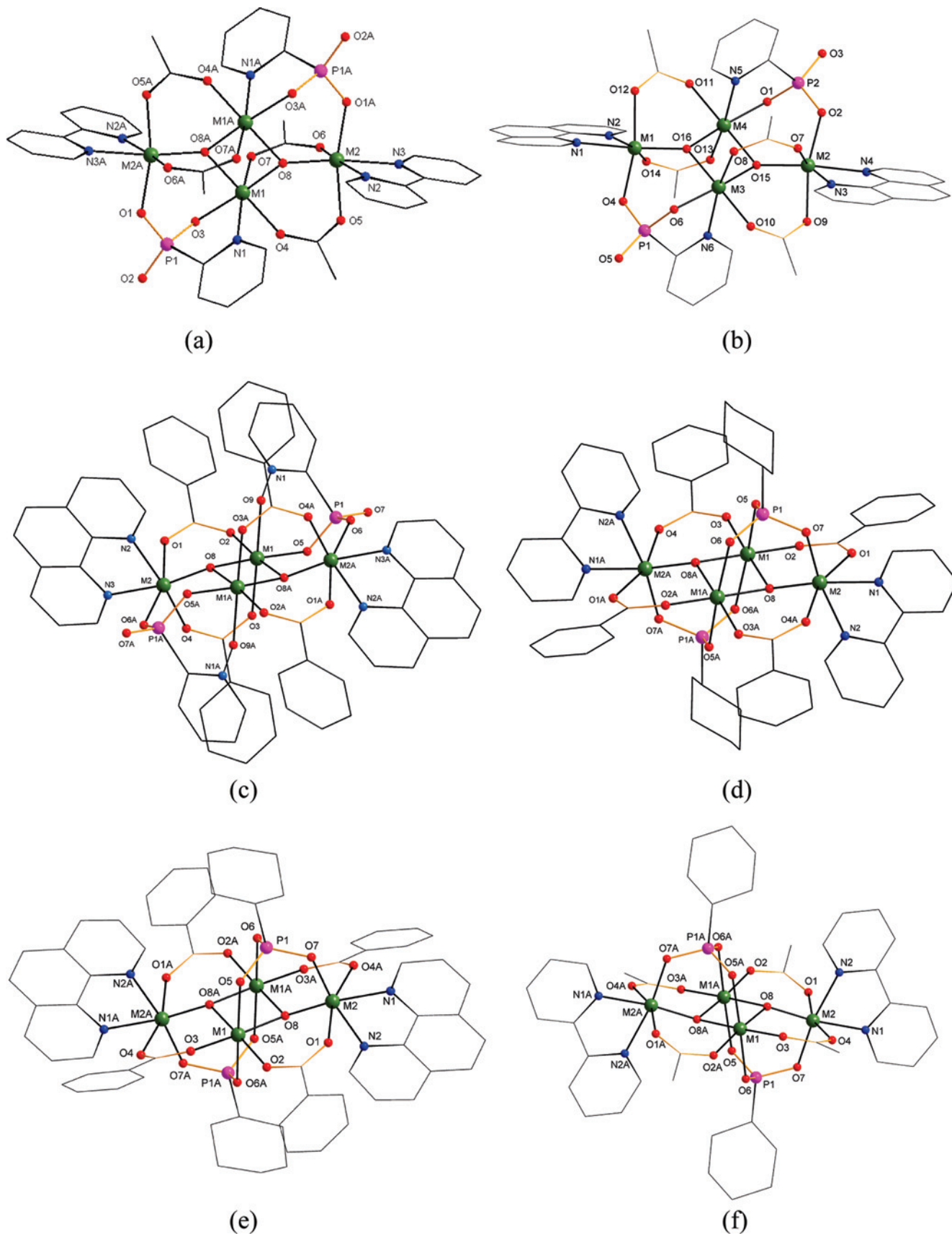


Figure 1. Molecular structures of compounds **1** (a), **2** (b), **3** (c), **4** (d), **5** (e), and **6** (f).

Each edge of the M_4 rhombus is bridged by either one O–P–O unit or two μ_2 -acetate groups. The $M_b \cdots M_w$ separations over the O–P–O and the acetate bridges are

3.494(2) Å for $M(1A) \cdots M(2)$ and 3.261(2) Å for $M(1) \cdots M(2)$, respectively. The $M_b \cdots M_b$ separation across the central O(8) atom [2.925(2) Å for $M(1) \cdots M(1A)$] is much shorter. The

Table 6. Comparison of Parameters of [Mn₃CrO₂]⁸⁺ Cores in **1–6**^a

	1	2	3	4	5	6
M _b •••M _b	2.925(2)	2.923(1)	2.929(1)	2.851(1)	2.848(2)	2.844(2)
M _b •••M _w	3.494(2)	3.457(1), 3.483(1)	3.368(1)	3.349(1)	3.343(2)	3.360(3)
M _b •••M _w	3.261(2)	3.249(1), 3.240(1)	3.273(1)	3.358(1)	3.346(2)	3.364(2)
M _b •••O _t	1.890(3)	1.890(3), 1.896(3)	1.926(1)	1.927(1)	1.914(2)	1.928(3)
M _b •••O _t	1.989(3)	1.922(2), 1.971(2)	1.947(1)	1.933(2)	1.931(2)	1.931(3)
M _w •••O _t	1.829(3)	1.854(2), 1.842(2)	1.808(1)	1.829(1)	1.832(2)	1.836(3)
M _b •••O _t •••M _b	97.9(1)	98.2(1), 100.2(1)	98.3(1)	95.2(1)	95.6(1)	94.9(2)
M _b •••O _t •••M _w	132.4(1)	132.6(1), 131.9(1)	127.5(1)	126.7(1)	126.3(1)	126.7(2)
M _b •••O _t •••M _w	122.6(1)	120.4(1), 120.2(1)	122.5(1)	125.8(1)	125.6(1)	126.2(2)
Δ	0.287	0.334, 0.280	0.370	0.376	0.380	0.375

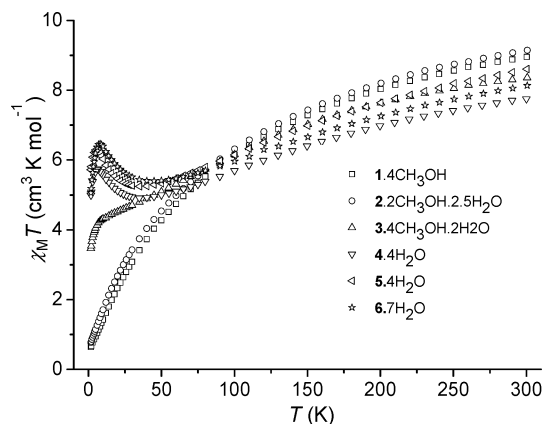
^a b = body, w = wingtip, t = triply-bridging, Δ = the distance of O_t to M₃ least-squares planes.

M_b–O–M_b and the M_b–O–M_w bond angles are 97.9(1)° for M(1)–O(8)–M(1A), 122.6(1)° for M(1)–O(8)–M(2), and 132.4(1)° for M(1A)–O(8)–M(2), respectively. The 2-pyridylphosphonate acts as a chelating and bridging ligand and links M(1) and M(2A) atoms using its pyridyl nitrogen [N(1)] and two phosphonate oxygen atoms [O(1) and O(3)]. The third phosphonate oxygen [O(2)] remains pendant [P(1)–O(2): 1.472(3) Å].

Complex **2**·2CH₃OH·2.5H₂O also crystallizes in the monoclinic *P2₁/c* space group. In this case, there are four crystallographically distinguished metal sites, each containing 3/4 Mn^{III} and 1/4 Cr^{III} (Figure 1b). Although the planar M₄O₂ core in the molecular structure of **2** is very similar to that in **1**, the corresponding bond lengths and angles are different (Table 3). The M–O and M–N bond lengths are 1.842(3)–2.105(3) Å and 2.056(3)–2.269(4) Å, respectively. The average M_b–O–M_b angle [99.2(1)°] is larger than that in **1** [97.9(1)°], while the average M_b–O–M_w angles [120.3(1), 132.3(1)°] are smaller than those in **1** [122.6(1), 132.4(1)°]. The average deviation of the central μ₃-O²⁻ from the M₄ plane is 0.310(2) Å, slightly larger than that in **1**. Obviously, the substitution of bipyridine in complex **1** by phenanthroline will cause significant changes in the structural parameters of the M₄O₂ core.

Such structural changes are also observed in compound **3**·4CH₃OH·2H₂O, where the 2-pyridylphosphonate and the acetate in **2** are replaced by (2-pyridyl-*N*-oxide)phosphonate and benzoate ligands (Table 4). As shown in Figure 1c, the coordination mode of (2-pyridyl-*N*-oxide)phosphonate in **3** is analogous to that of 2-pyridylphosphonate in **2**. It behaves as a chelating and bridging ligand and links the M(1) and M(2A) atoms with the M_b–O–M_b angle of 98.3(1)°, while the M_w–O–M_b angles are 122.4(2) and 127.5(1)°. The deviation of the central μ₃-O²⁻ from the M₄ plane is 0.370(2) Å, larger than that in **2**.

If we replace the 2-pyridylphosphonate or (2-pyridyl-*N*-oxide)phosphonate in **1–3** by a cyclohexanephosphonate ligand, complexes **4–6** are obtained, which contain similar planar M₄O₂ cores (Figures 1d–f). In the latter cases, however, each cyclohexanephosphonate ligand caps on top of the M₃O triangle and links to three M^{III} ions by using its three phosphonate oxygen atoms. Consequently, compared with those in **1–3**, the M_b•••M_b distances [2.851(1) Å for **4**, 2.848(2) Å for **5**, and 2.844(2) Å for **6**] are shortened, and the M_b–O–M_b angles [95.2(1)° for **4**, 95.6(1)° for **5**, and 94.9(2)° for **6**] are significantly reduced. The deviations of the central oxygen atoms from the M₄ planes are 0.376(1),

**Figure 2.** $\chi_M T$ versus T plot for compounds **1–6**.

0.380(1), and 0.375(3) Å for **4**, **5**, and **6**, respectively. Table 6 compares the structural parameters of the M₄O₂⁸⁺ cores in complexes **1–6**.

It could be of interest to compare structures **4–6** with those of homonuclear manganese(III) complexes [Mn₄O₂-(O₂CCH₃)₄(O₃PC₆H₁₁)₂(phen)₂] and [Mn₄O₂(O₂CPh)₄(O₃PC₆H₁₁)₂(bpy)₂], in which the same cyclohexanephosphonate ligand is employed.²⁶In the latter cases, the Mn_b•••Mn_b distances are 2.851 and 2.863 Å, respectively. The Mn_b–O–Mn_b angles are 96.2(2) and 96.0(1)°, respectively. These parameters are close to those for complexes **4–6**.

Magnetic Properties. Solid state dc magnetic measurements were performed on **1–6** in the temperature range 1.8–300 K in a field of 2 kG. The $\chi_M T$ versus T plots are shown in Figure 2. At 300 K, the $\chi_M T$ values are 8.95, 9.14, 8.36, 7.75, 8.61, and 8.14 cm³ K mol⁻¹ for compounds **1–6**, respectively, lower than the calculated spin-only value (10.875 cm³ K mol⁻¹) for three Mn^{III} ($S = 2$) and one Cr^{III} ($S = 3/2$) ions, indicating an appreciable antiferromagnetic exchange between the magnetic centers in compounds **1–6**.

For compounds **1–3**, the $\chi_M T$ values decline monotonously and reach 0.65, 0.77, and 3.47 cm³ K mol⁻¹ at 1.8 K for **1**, **2**, and **3**, respectively. For compounds **4–6**, a minimum appears at 40 K for **4** (4.92 cm³ K mol⁻¹), 35 K for **5** (5.25 cm³ K mol⁻¹), and 45 K for **6** (5.40 cm³ K mol⁻¹), respectively. Below these temperatures, the $\chi_M T$ values increase and approach maxima of 5.74, 6.31, and 6.46 cm³ K mol⁻¹ at 7, 6, and 8 K before decreasing rapidly to 4.99,

(26) Ma, Y.-S.; Yao, H.-C.; Hua, W.-J.; Li, S.-H.; Li, Y.-Z.; Zheng, L.-M. *Inorg. Chim. Acta* **2007**, *360*, 1645.

5.72, and 5.06 $\text{cm}^3 \text{K mol}^{-1}$, respectively, at 1.8 K. This behavior suggests that net magnetic moments arise from the competing magnetic interactions of the metal ions in compounds 4–6. Further decreasing of $\chi_M T$ at lower temperature could be due to the zero-field splitting of the ground state and/or the intercluster antiferromagnetic interactions.

The different magnetic behaviors of 4–6 from those of 1–3 should originate from their structures. As already discussed, compounds 1–6 have similar M_4O_2 planar cores with two distinct coordination sites, inner site (M_b) and outer site (M_w), but the position of a single Cr^{III} ion cannot be assigned from their structures. From this viewpoint, these compounds may be regarded as Cr-doped materials of the corresponding homo- Mn_4 clusters. A discussion on the magnetostructural correlation of these complexes thus becomes very difficult. Nevertheless, a comparison of the structural parameters of complexes 1–6 could help us in understanding their magnetic behaviors. It is found that, despite the similar M_4O_2 planar cores in all cases, the bond lengths and angles within the M_4O_2 core vary when the peripheral ligands (e.g., the carboxylates, phosphonates, or chelating ligands) change. The change is especially significant when the coordination modes of the phosphonate ligands are different. For complexes 1–3, both 2-pyridylphosphonate and (2-pyridyl-*N*-oxide)phosphonate chelate and bridge to two metal atoms (M_b and M_w). The $\text{M}_b \cdots \text{M}_b$ distances and the $\text{M}_b\text{—O—M}_b$ angles are approximately 2.92 Å and 98–99°, respectively. While in complexes 4–6, each cyclohexanephosphonate caps on top of the M_3O triangle and links to three M^{III} ions. The $\text{M}_b \cdots \text{M}_b$ distances and the $\text{M}_b\text{—O—M}_b$ angles become approximately 2.85 Å and 95°, respectively. In these cases, the antiferromagnetic interactions between the inner atoms (M_b) may be remarkably weakened compared with those in complexes 1–3. Hence, net magnetic moments arise from the competing interactions within the tetranuclear M_4O_2 core. Monotonous decrease of the $\chi_M T$ values upon cooling was also observed in complexes $[\text{Mn}_4\text{O}_2(\text{O}_2\text{CCH}_3)_4(\text{O}_3\text{PC}_6\text{H}_{11})_2(\text{phen})_2]$ and $[\text{Mn}_4\text{O}_2(\text{O}_2\text{CPh})_4(\text{O}_3\text{PC}_6\text{H}_{11})_2(\text{bpy})_2]$, which possess similar core structures to those of 4–6.²⁶ Apparently, the dope of Cr^{III} to the homo- Mn_4 clusters poses influences on their magnetic properties.

The change in structural parameters may also vary their ground-state spins. For a complex containing three Mn^{III} and one Cr^{III} , the total spin values range from $1/2$ to $15/2$. In order to determine the ground-state spin, magnetization data were collected in the temperature range 1.8–10 K and the dc magnetic field range 10–70 kG for complexes $5 \cdot 4\text{H}_2\text{O}$ and $6 \cdot 7\text{H}_2\text{O}$. Figure 3 shows the $M/N\beta$ versus H/T curve for complex $5 \cdot 4\text{H}_2\text{O}$. The nonsuperimposable isofields would suggest significant zero-field splitting in the spin ground state. Unfortunately, our efforts to obtain the zero-field splitting parameter (D) from the $M/N\beta$ versus H/T curves were not successful, possibly due to the population of low-lying excited states at temperatures down to 1.8 K.^{27,28}

Alternating current magnetization measurements were performed on $5 \cdot 4\text{H}_2\text{O}$ in the 1.8–6 K range in a 5 G ac field oscillating at 1–1488 Hz (Figure 4). Both the in-

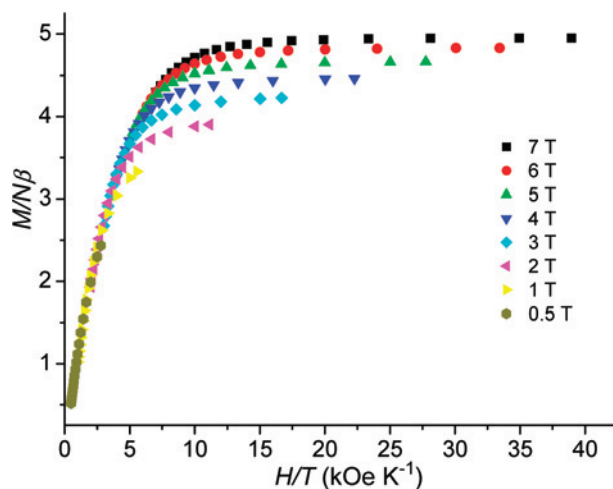


Figure 3. $M/N\beta$ vs H/T plot for $5 \cdot 4\text{H}_2\text{O}$.

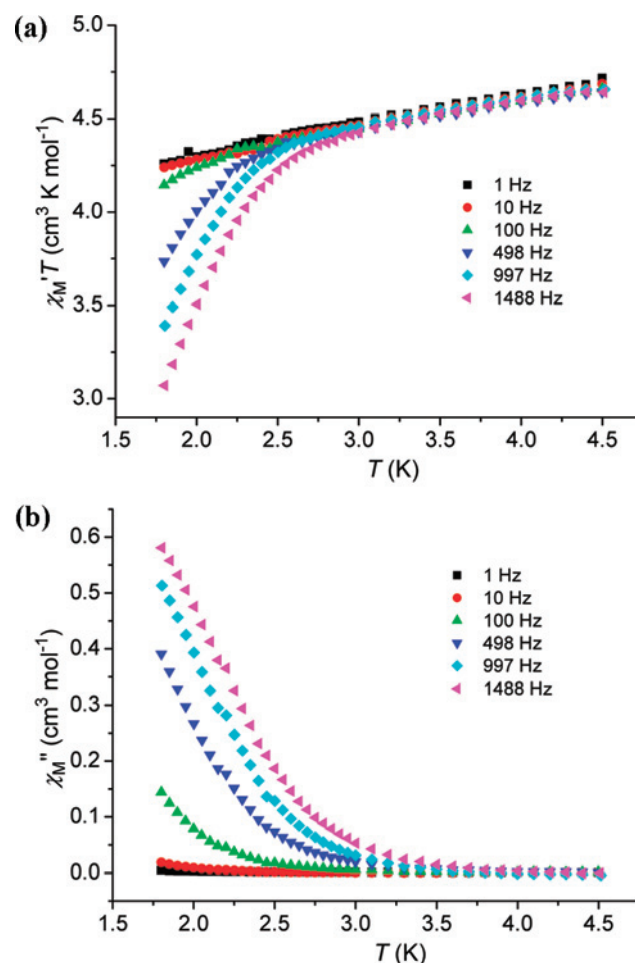


Figure 4. Plots of $\chi'T$ (top) and χ'' (bottom) vs T for compound $5 \cdot 4\text{H}_2\text{O}$.

phase and out-of-phase signals are frequency-dependent, indicating a slow magnetic relaxation below approximately 4.0 K. This behavior corresponds to a slow kinetics of

(27) Murugesu, M.; Raftery, J.; Wernsdorfer, W.; Christou, G.; Brechin, E. K. *Inorg. Chem.* **2004**, *43*, 4203.

(28) (a) Rajaraman, G.; Murugesu, M.; Sañudo, E. C.; Soler, M.; Wernsdorfer, W.; Helliwell, M.; Muryn, C.; Raftery, J.; Teat, S. J.; Christou, G.; Brechin, E. K. *J. Am. Chem. Soc.* **2004**, *126*, 15445. (b) Sañudo, E. C.; Wernsdorfer, W.; Abboud, K. A.; Christou, G. *Inorg. Chem.* **2004**, *43*, 4137. (c) Scott, R. T. W.; Milios, C. J.; Vinslava, A.; Lifford, D.; Parsons, S.; Wernsdorfer, W.; Christou, G.; Brechin, E. K. *Dalton Trans.* **2006**, 3161.

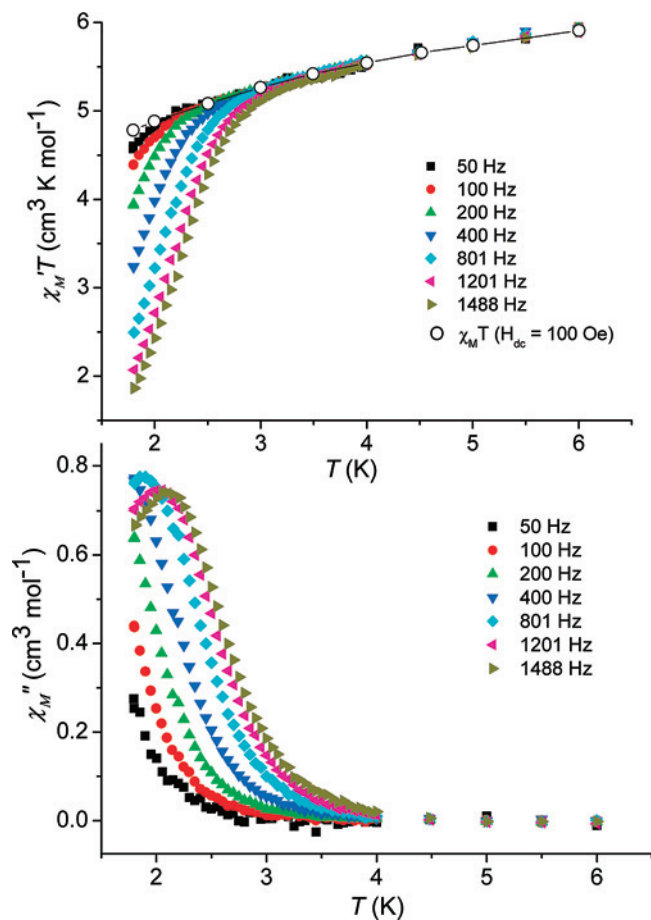


Figure 5. Plots of $\chi' T$ (top) and χ'' (bottom) vs T for compound $6 \cdot 7\text{H}_2\text{O}$. The dc data measured at 100 Oe is also shown for comparison.

magnetization reversal relative to the ac oscillation frequencies and is often associated with the phenomenon of single-molecule magnet.²⁹ The $\chi_M' T$ versus T plot above 3.5 K does not display a plateau, suggesting that excited states are still populated at these low temperatures.³⁰ Extrapolation of the $\chi_M' T$ signal from values above 3.5 K gives $4.3 \text{ cm}^3 \text{ K mol}^{-1}$ at 0 K, suggesting a spin ground state of $S = 2.5$ for $5 \cdot 4\text{H}_2\text{O}$.

The temperature-dependent ac magnetic susceptibilities for compound $6 \cdot 7\text{H}_2\text{O}$ are given in Figure 5. Again, both the in-phase and out-of-phase signals are frequency-dependent below approximately 4 K, indicative of slow magnetic relaxation below this temperature. No plateau is observed in the $\chi_M' T$ versus T plot above 3.5 K, suggesting the population of excited states at these low temperatures. This may explain our failure in fitting the $M/N\beta$ versus H/T curve for compound $6 \cdot 7\text{H}_2\text{O}$ (Figure 6). Extrapolation of the $\chi_M' T$ versus T plot to 0 K gives a $\chi_M' T$ value of $4.5 \text{ cm}^3 \text{ K mol}^{-1}$, in agreement with an $S = 2.5$ ground state with $g = 2.0$. The out-of-phase signal (χ_M'') shows peaks above 1.8 K, which shift to high temperature with increasing frequencies, characteristic for

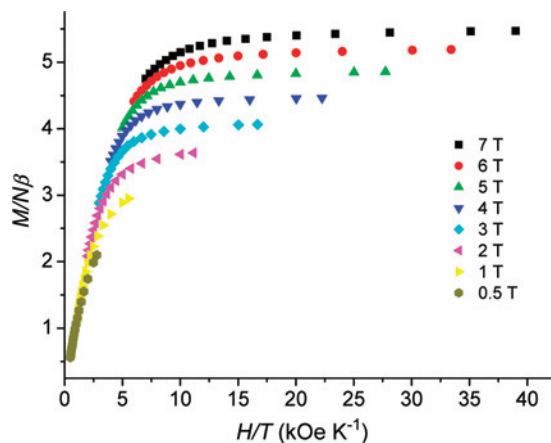


Figure 6. $M/N\beta$ vs H/T plot for $6 \cdot 7\text{H}_2\text{O}$.

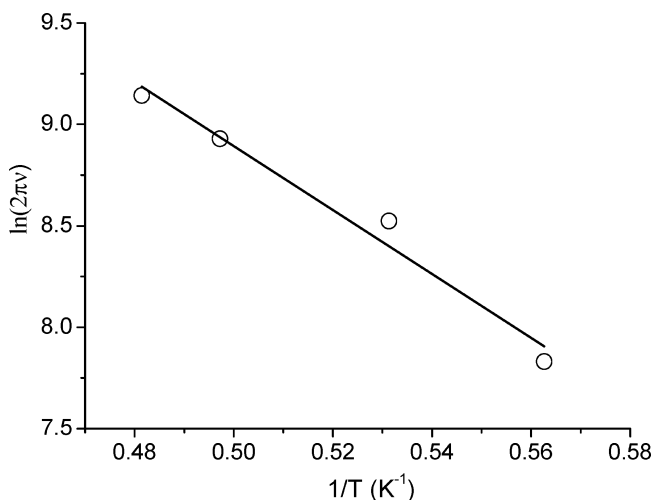


Figure 7. Least-squares fit (solid line) of the experimental data to the Arrhenius equation for $6 \cdot 7\text{H}_2\text{O}$.

a single-molecule magnet. The peak temperature at a fixed frequency may be obtained by the Lorentz peak function fitting. This makes it possible to fit the ac data by the Arrhenius equation: $\tau = \tau_0 e^{-\Delta E/k_B T}$, where τ is relaxation time, ΔE is the activation energy, k_B is the Boltzmann constant, and τ_0 is the preexponential factor. The slope of the Arrhenius plot gives the following parameters: $\Delta E/k_B = 15.76 \text{ K}$ and $\tau_0 = 5.21 \times 10^{-8} \text{ s}$ (Figure 7).

Conclusion

In this paper, we develop a new synthetic route, by using $(\text{NBu}_4)_2\text{Cr}_2\text{O}_7$ to oxidize Mn^{II} in situ, and succeed in producing six new heteronuclear $\text{Mn}^{\text{III}}/\text{Cr}^{\text{III}}$ complexes **1–6** with a general formula $[\text{Mn}_3\text{CrO}_2(\text{O}_2\text{CR}^1)_4(\text{O}_3\text{PR}^2)_2(\text{L})_2]$ ($\text{R}^1 = \text{CH}_3, \text{Ph}$; $\text{R}^2 = \text{C}_5\text{H}_4\text{N}, \text{C}_5\text{H}_4\text{NO}, \text{C}_6\text{H}_{11}$; $\text{L} = \text{bpy}, \text{phen}$). These compounds contain similar $[\text{Mn}_3\text{CrO}_2]^{8+}$ cores with the four metal sites arranged in planar topologies. Although we are not able to identify the Cr and Mn sites in the cores at this stage, systematic changes in the structural parameters are observed when the peripheral ligands such as the carboxylate, phosphonate, and chelating ligands are changed. More interestingly, the structural changes are reflected by their magnetic properties. In the cases of compounds **5** and **6**, slow magnetization relaxations characteristic of single-

(29) Rumberger, E. M.; Shah, S. J.; Beedle, C. C.; Zakharov, L. N.; Rheingold, A. L.; Hendrickson, D. N. *Inorg. Chem.* **2005**, *44*, 2742.

(30) Boskovic, C.; Brechin, E. K.; Streib, W. E.; Foltling, K.; Bollinger, J. C.; Hendrickson, D. N.; Christou, G. *J. Am. Chem. Soc.* **2002**, *124*, 3725.

molecule magnet behaviors are observed. The ground states are $S = 2.5$ for both **5** and **6**.

Acknowledgment. We thank the NSF of China (No. 20325103, 20631030, 20721002), the National Basic Research Program of China (2007CB925102), and 111 Project under Grant No. B07026 for financial support.

Supporting Information Available: X-ray crystallographic files in CIF format for the six compounds, selected bond lengths and angles for compounds **1–6**, and $\chi_M T$ versus T plots and hysteresis measurements for compound **6**. This material is available free of charge via the Internet at <http://pubs.acs.org>.

IC701626K